

Numerical Simulation of Tire Reinforced Sand Behind Retaining Wall Under Earthquake Excitation

Amina Lazizi

Civil Engineering Dpt,
Djillali Liabes University of
Sidi Bel Abbes, Algeria
lazizi_a18@yahoo.fr

Habib Trouzine

LGCE Laboratory, Djillali
Liabes University of Sidi Bel
Abbes, Algeria
h_trouzine@yahoo.fr

Aissa Asroun

LGCE Laboratory, Djillali
Liabes University of Sidi Bel
Abbes, Algeria
a_asroun@yahoo.fr

Farid Belabdelouahab

ENSTP National High
School of Publics Work,
Kouba, Algiers, Algeria
belabdelouahabf@yahoo.fr

Abstract—This paper studies the numerical simulations of retaining walls supporting tire reinforced sand subjected to El Centro earthquake excitation using finite element analysis. For this, four cases are studied: cantilever retaining wall supporting sand under static and dynamical excitation, and cantilever retaining wall supporting waste tire reinforced sand under static and dynamical excitation. Analytical external stability analyses of the selected retaining wall show that, for all four cases, the factors of safety for base sliding and overturning are less than default minimum values. Numerical analyses show that there are no large differences between the case of wall supporting waste tire reinforced sand and the case of wall supporting sand for static loading. Under seismic excitation, the higher value of Von Mises stress for the case of retaining wall supporting waste tire reinforced sand is 3.46 times lower compared to the case of retaining wall supporting sand. The variation of horizontal displacement (U1) and vertical displacement (U2) near the retaining wall, with depth, are also presented.

Keywords- waste tire; sand; retaining wall; earthquake; simulation

I. INTRODUCTION

With the rapid growth in automobile usage worldwide, approximately 2–3 billion tires are discarded annually [1-2]. Algeria alone produces approximately 25918.50 tons/year of used tires [3]. The most common ways to recycle tires are burying, auxiliary fuel conversion, pyrolysis, reproduction, cutting and reprocessing, and reusing. Applications in geotechnical engineering, highway engineering, soil and water conservation, and marine engineering use intact used tires. Such applications which do not require complex processes are considered economical and eco-friendly [4-6].

The first research in France on soil reinforcements using old tires was commissioned in 1976. Studies were conducted on reinforcement in the form of whole tires, sidewalls, or treads placed on edge or cut and laid flat [4-7]. The first project in England using scrap tires was the construction of an experimental gravity wall in West Yorkshire [8]. An experimental research using a vibrating table was also undertaken from the “l’Ecole Nationale des Ingénieurs de

Tunis” (ENIT) and the “Laboratoire Centrale des Ponts et Chaussées” (LCPC), whose objective was to protect the Grenoble synchrotron road from vibrations. This study showed that used tires can attenuate vibration phenomena [9]. Another full-scale experimentation was conducted in Rouen in France; this research showed that tire reinforced soil can absorb and reduce pressure and acceleration [10].

In the seismic stability analysis, the magnitude of the dynamic force increment due to shaking is calculated using the Mononobe-Okabe (M.O) approach [11]. Basha and Babu in [12] presented a method to evaluate the internal stability of reinforced soil structures against tension and pullout modes of failures using pseudo-static methods for earthquake conditions. Further, Choudhury and Ahmed in [13] presented the external stability of waterfront reinforced soil structures under seismic conditions using a pseudo-static method and a limited equilibrium approach. Steedman and Zeng in [14] developed the pseudo-dynamic method considering horizontal seismic acceleration and finite shear waves propagations using planar failure surface.

In the present paper, a numerical simulation of tire reinforced sand behind retaining wall under earthquake using implicit and explicit methods is performed in order to study its dynamic behavior.

II. DESCRIPTION OF THE NUMERICAL MODEL

A. Geometry and ground conditions

Geometrically, the retaining wall is a reinforced concrete cantilever wall with 5.80 m of height and 0.50 m of wall stem thickness (Figure 1). Mechanically, the Young’s modulus of the retaining wall is $E=3.107 \text{ kN/m}^2$, the Poisson’s ratio is about 0.3 and its density is about 26.43 kN/m^3 . Table I summarizes all the characteristics. The earthfill is a sandy soil with a semi-infinite length of 22.50 m. The surface of the backfill is plane and carries no surcharge. The seismic action is introduced in the form of the accelerogram acquired from the earthquake dated May 18, 1940 in El Centro in the region of California.

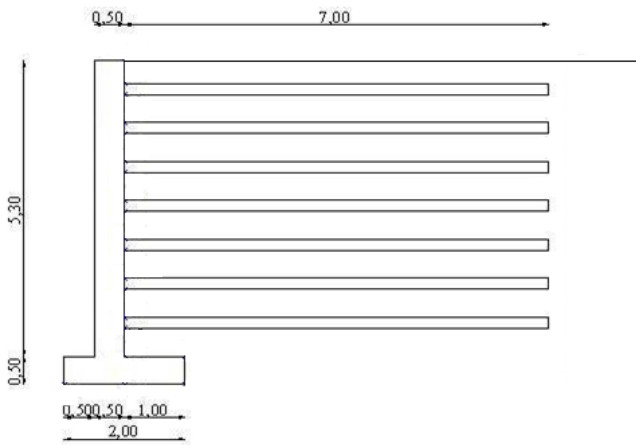


Fig. 1. Geometric details of the wall.

TABLE I. MODEL CHARACTERISTICS

Materials	Properties
Retaining Wall	$E_w = 3.E+7 \text{ kN/m}^2$ $\nu_w = 0.25$ $\rho_w = 26\,430 \text{ kg/m}^3$ damping $\alpha = 0.015$
Sand	$E_s = 100\,000 \text{ kN/m}^2$ $\nu_s = 0.25$ $\rho_s = 18\,260 \text{ kg/m}^3$ damping $\alpha = 0.01$
Tire reinforced Sand	$E_t = 100\,000 \text{ kN/m}^2$ $\nu_t = 0.25$ $\rho_t = 17\,940 \text{ kg/m}^3$ damping $\alpha = 0.02$

B. Studied cases

Two distinct cases are studied; a reference case where the wall supports only the sand and a second case where the sand is reinforced by layers of waste tires. Both cases are studied under static and dynamic loading.

1) Case 1 : Retaining wall supporting sand

The backfill is wet sand with an average diameter of 1.10 mm, a density of 26.5 kN/m³, and a coefficient of curvature about 0.119 to 0.136. According to the unified classification (USCS), the soil is SP poorly graded clean sand. Geotechnically, the cohesion is zero, and the angle of internal friction is 30°. Mechanically, the Young’s modulus E is 1.105 kN/m², the Poisson’s ratio is about 0.25 and its density is 18.40. The active earth pressure coefficient is determined using the Rankine method, and it is about 0.333. The wall slip is considered with a coefficient of friction of 0.4.

2) Case 2 : Retaining wall supporting tire reinforced sand

In this case, the same sand is reinforced with layers of light vehicle tires type flanks without treads on edge. The composite (tire-sand) is amended as multi layer, its Young modulus and Poisson’s ratio are determined using Voigt Reuss combined model:

$$E_{C-VR} = E_m \cdot \beta / \gamma \quad (1)$$

$$\beta = E_m + V_a^{2/3} (E_a - E_m) \quad (2)$$

$$\gamma = \beta \left(1 - V_a^{1/3} \right) + \left(E_m \cdot V_a^{1/3} \right) \quad (3)$$

with:

E_{C-VR} : the Equivalent Young’s modulus

E_m, E_a : the Sand and Waste Tire Young moduli

$$V_a = \frac{V_c}{V_c + V_s} \quad \text{with } V_c, V_s : \text{the sizes of tire and sand}$$

The tire height is 20 cm, and the layer of sand is 50 cm. The reinforcements are linear modeled as a superposition of the layer of sand and waste tire. The sand-rubber interaction is considered with a coefficient of sliding friction of 0.6; the rubber-wall friction coefficient is equal to 0.65. The active earth pressure coefficient is computed the same way as in the first case.

III. STATIC AND SEISMIC LOADING

For static loading, the weight of retaining wall is computed, and the active pressure is calculated using the Rankine method and is about 86 kN in the first case and 85.4 kN in the second case. For seismic loading, the accelerogram of the El Centro Earthquake in California is introduced in the form of a table of two columns, the first for time, which is limited in 14 s, and the second for the values of acceleration [15]. Rayleigh mass proportional damping factor is introduced for each element (wall, soil and tire-soil).

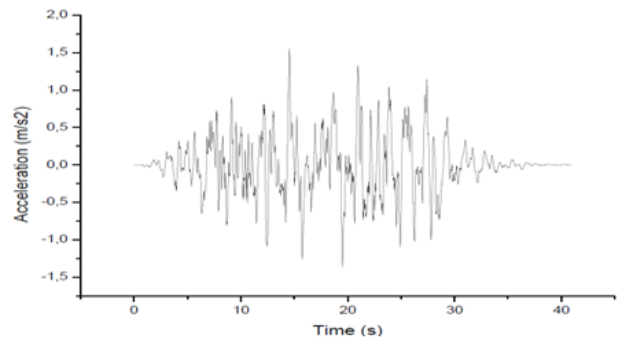


Fig. 2. The accelerogram of El Centro California

IV. RESULTS AND DISCUSSION

A. External stability analyses

To calculate the lateral earth pressure, Rankine’s theory is used. For the dynamic case the calculation is based on the pseudo-static method.

1) Base sliding-Static case

The coefficient of Rankine active earth pressure is given by:

$$K_a = \tan^2 (45 - \phi/2) \quad (4)$$

where K_a is the active earth pressure coefficient and ϕ is the angle of soil internal friction. The static earth pressure is given by:

$$P_a = 0.5 K_a \gamma_t H^2 \quad (5)$$

where P_a is the static earth pressure and γ_t and H are respectively the total unit weight of backfill soil and the height of the retaining wall.

The sliding resistance is provided by the friction between the concrete and the soil under the base of the wall. The frictional force between the concrete and the soil is computed using the following equation:

$$F_f = R_v \tan \delta \quad (6)$$

where F_f is the frictional force between the concrete and the soil, R_v is the vertical component of resultant force. F_r is the force opposing the sliding and:

$$F_r = F_f \quad (7)$$

$$R_v = W_{Total} \quad (8)$$

where W_{Total} is the resultant weight of the wall.

The safety factor against sliding is equal to:

$$F_s = F_r / P_a \quad (9)$$

2) Base sliding - Dynamic case

The pseudostatic earthquake force is given by [16]:

$$P_e = \frac{3 a_{max}}{8g} (\gamma_t H^2) \quad (10)$$

where P_e is the pseudostatic earthquake force and a_{max} is the peak ground acceleration and:

$$P_{ae} = P_a + P_e \quad (11)$$

where P_{ae} is the sum of the static (P_a) and the pseudo-static earthquake force (P_e).

The safety factor for sliding using both pseudostatic method and Seed and Whitman (1970) analysis is given by:

$$F_s = \frac{N \tan \delta_1}{P_h + P_e} \quad (12)$$

where N is the sum of the weight of wall, the footing and the vertical component of the active earth pressure resultant force, δ_1 is the friction between the bottom of the foundation and the soil backfill, and P_h is the horizontal component of the active earth pressure resultant force with:

$$N = W + P_a \sin \delta \quad (13)$$

$$P_h = P_a \cos \delta \quad (14)$$

3) Overturning - Static case

The overturning and stabilizing moments may be calculated by taking moments about point O. The safety factor against overturning is therefore:

$$F_{sr} = \frac{M_{st}}{M_r} \quad (15)$$

where M_{st} is the sum of moments that resist overturning and M_r is the sum of overturning moments.

4) Overturning - Dynamic case

The safety factor for overturning using Mononobe-Okabe method is given as:

$$F_s = \frac{W \cdot a}{0.333 P_{ae} H \cos \delta - e P_{ae} \sin \delta} \quad (16)$$

where a the lateral distance from resultant weight W of wall and footing to toe of footing, H the height of the retaining wall and e the lateral distance from the vertical component of the active earth pressure resultant force to the toe of wall with:

$$P_v = P_a \sin \delta \quad (17)$$

where P_{ae} is the sum of the static (P_a) and the pseudostatic earthquake force (P_e).

If the conventional rule is applied, according to which the dynamic safety factor should not be less than 75%, the safety factor for sliding as well as for overturning should be in the range of 1.1 to 1.2.

V. NUMERICAL ANALYSES

The finite element method (FEM) has become the most popular method in both research and industrial numerical simulations. Several algorithms, with different computational costs can be implemented in ABAQUS [17], which is a commonly used software for finite element analysis. Understanding the nature, advantages and disadvantages of these algorithms is very helpful for choosing the right algorithm for a particular problem [18]. Comparison of implicit and explicit methods for ABAQUS in nonlinear problems has been reported by Rebelo in [19]. The unconditionally stable implicit method will encounter some difficulties when a complicated three dimensional model is considered. The reasons are as follows [18]: as the reduction of the time increment continues, the computational cost in the tangent stiffness matrix is dramatically increased and even causes divergence. Local instabilities cause force equilibrium to be difficult to achieve.

Explicit techniques are thus introduced to overcome the disadvantages of implicit methods. For the explicit method, the CPU cost is approximately proportional to the size of the finite element model and does not change as dramatically as the implicit method. The drawback of the explicit method is that it is conditionally stable. The stability limit for an explicit operator is that the maximum time increment must be less than a critical value of the smallest transition times for a dilatational wave to cross any element in the mesh. Secondly, the nature of the explicit method limits it to the analysis of short transient problems. If this method is used for quasi-static problems, the inertia effects must be small enough to be neglected. One way to assure this is to set the limit of the kinematic energy to be less than 5% of the strain energy. For dynamic problems, ABAQUS also offers some other methods such as a modal

dynamic algorithm. However, only direct integration methods implicit dynamics and explicit methods are suitable for nonlinear problems. Most of the reported works on the comparison of implicit and explicit methods are on quasi-static nonlinear problems [18-20].

As it is well-known, the explicit integration operator is conditionally stable since the maximum stable time increment is limited by the minimum mesh size and the highest wave speed (Courant stability condition) given by [21-22]:

$$\Delta t \leq \min (l_e / C_d)$$

where l_e is the characteristic element length (e.g. minimum element dimension) and C_d is the current effective, dilatational wave speed of the material. In other words, the time increment must be smaller than the minimum amount of time necessary for a wave to cross an element. The time step of $T = 2.2 \cdot 10^{-4}$ s has been found to be sufficiently powerful in obtaining an effective approximate computations of the quasi-static response [23].

It should be mentioned that the values of damping for each material is regrouped in Table I. To get a clear comparison of the Von Mises stress distributions for the four studied cases, the Von Mises stress distributions are shown in Figures 3, 4, 5 and 6.

A. Retaining wall supporting sand - Static case:

According to the analytical computation, for this case, the safety factors for sliding as well as overturning are less than the default minimum values.

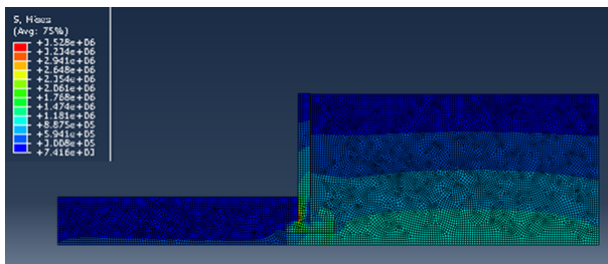


Fig. 3. The Von Mises stress distribution for retaining wall supporting sand under static loading

Von Mises stress distribution change in the range of 7.416–3528 kPa (Figure 3). The lowest Von Mises stress values are observed near the ground level. Von Mises stress increases with depth. The higher Von Mises stress (3.5 MPa) is observed between the base slab and the stem of the retaining wall in the soil cover zone. Figure 7 presents U1 and U2 displacements under static loading for the two studied cases. Variations of U1 and U2 displacements of the wall with depth are presented in Figures 9 and 10. Case 1 and 2 make reference respectively to retaining wall supporting sand and retaining wall supporting reinforced sand. The displacement U1 is substantially constant with the depth (about 0.825 m). For U2 the maximum value is noted in the base slab and it's about 0.0065 m. The minimum value is noted in the top of the wall and it's about 0.0025 m.

Figure 5 presents the Von Mises stress distribution at 14 seconds (after 1023 time increments). For the second case, Von Mises stress distribution change in the range of 9.761 kPa to 13.95 MPa. The lowest Von Mises stress values (9.7 kPa) for this case are observed for backfill. The higher Von Mises stress (13.95 MPa) is observed in the wall between the base slab and the stem. The higher value of Von Mises stress for the dynamical case is 3.95 time higher than for the static case.

Figure 8 presents U1 and U2 displacements under static loading for the two studied cases. Variations of U1 and U2 displacements with depth are presented in Figure 11 and Figure 12. U1 displacement is about 0.70 m for all the depth. For U2 displacement, the maximum value is about 0.0053 m and the minimum value is about 0.002 m.

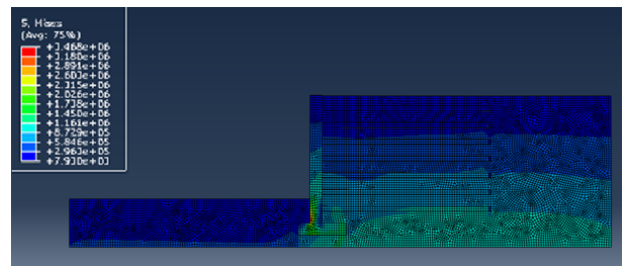


Fig. 4. The Von Mises stress distribution for retaining wall supporting Tire-reinforced sand under static loading

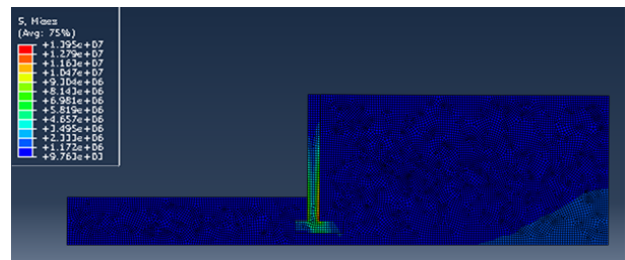


Fig. 5. The Von Mises stress distribution for retaining wall supporting sand under seismic loading

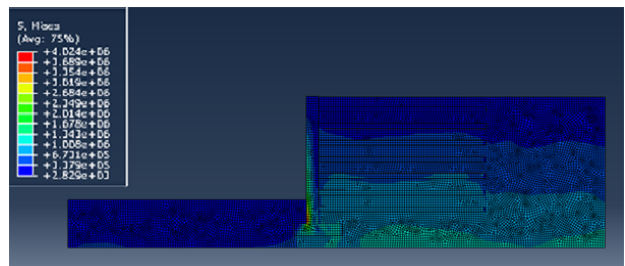


Fig. 6. The Von Mises stress distribution for retaining wall supporting tire-reinforced sand under seismic loading

B. Retaining wall supporting sand - Dynamic case:

According to the analytical computation, for this case, the safety factors for sliding as well as overturning are greater than the default minimum values.

C. Retaining wall supporting tire reinforced sand - Static case:

According to the analytical computation, for this case, the safety factors for sliding as well as overturning are less than the default minimum values.

For the third case, the Von Mises stress distribution change in the range of 7.930 to 3465 kPa (Figure 4). The lowest Von Mises stress values are observed near the ground level. Von Mises stress increases with depth. The higher Von Mises stress

is observed between the base slab and the stem of the retaining wall in the soil cover zone. There are not large differences between this case and the case of wall supporting sand for static loading.

Figure 7 presents U1 and U2 displacements under static loading for the two studied cases. Variations of U1 and U2 displacements with depth are presented in Figures 9 and 10. The value of U1 for this case is about 0.625 m, for U2 displacement the maximum value is about 0.005 m.

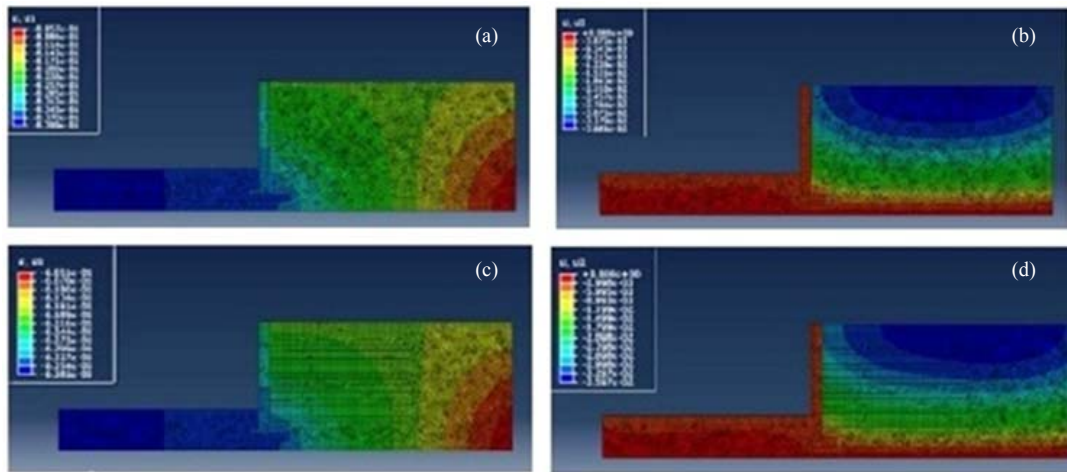


Fig. 7. Displacements under static loading (a) U1 displacement for retaining wall supporting sand. (b) U2 displacement for retaining wall supporting sand. (c) U1 displacement for retaining wall supporting Tire-reinforced sand. (d) U2 displacement for retaining wall supporting Tire-reinforced sand

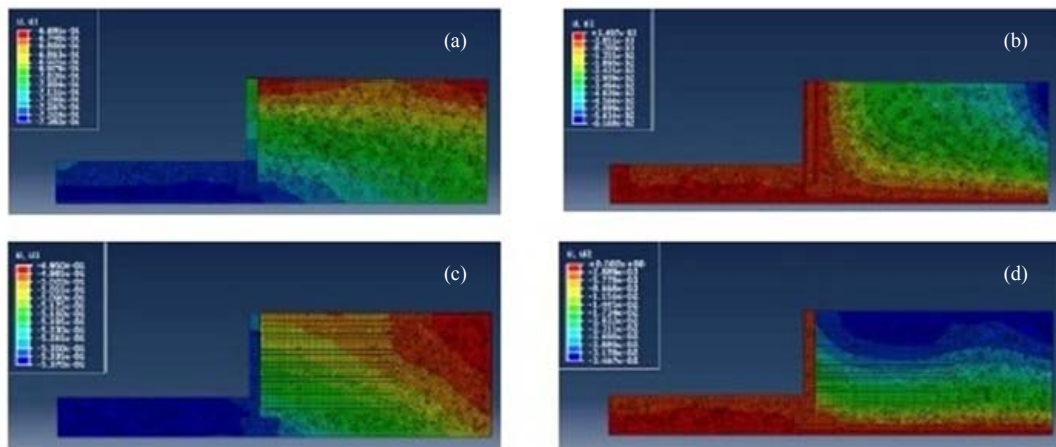


Fig. 8. Displacements under seismic loading (a) U1 displacement for retaining wall supporting sand. (b) U2 displacement for retaining wall supporting sand. (c) U1 displacement for retaining wall supporting Tire-reinforced sand. (d) U2 displacement for retaining wall supporting Tire-reinforced sand

D. Retaining wall supporting tire reinforced sand - Dynamic case:

Figure 6 presents the Von Mises stress distribution at 14 seconds (after 3869 time increments). For the fourth case, the Von Mises stress distribution change in the range of 2.829 kPa to 4.024 MPa. The lowest Von Mises stress values are observed near the ground level. Von Mises stress increases

with depth. The higher Von Mises stress is observed between the base slab and the stem of the retaining wall in the soil cover zone. The higher value of Von Mises stress for this case is 3.46 times lower compared to the case of the retaining wall supporting sand with dynamic loading.

Figure 8 presents U1 and U2 displacements under static loading for the two studied cases. Variations of U1 and U2 displacements with depth are presented in Figures 11 and 12.

The U1 displacement is about 0.50 m and U2 displacement is about 0.0048 m.

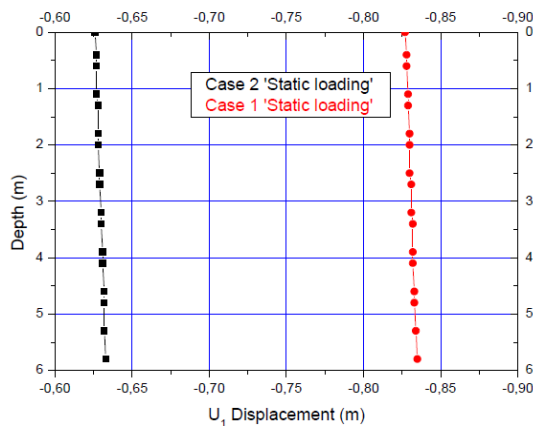


Fig. 9. Variation of U1 wall displacement with depth for static loading

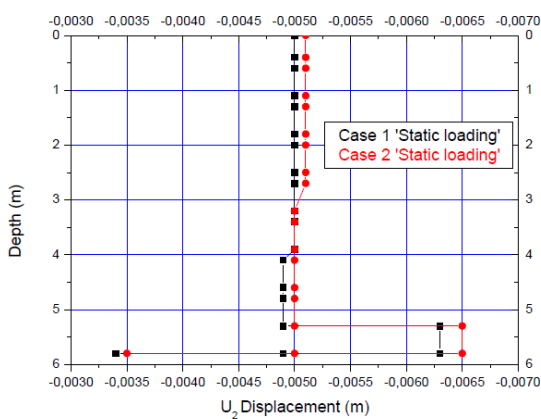


Fig. 10. Variation of U2 wall displacement with depth for static loading

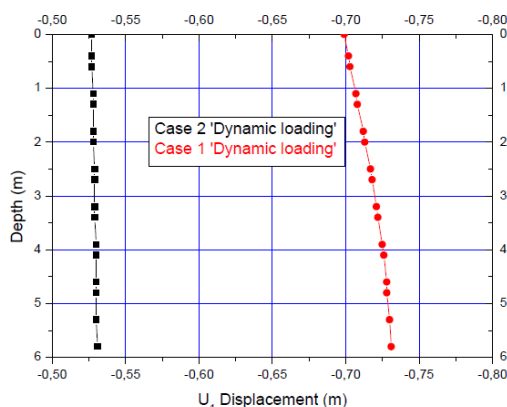


Fig. 11. Variation of U1 wall displacement with depth for seismic loading.

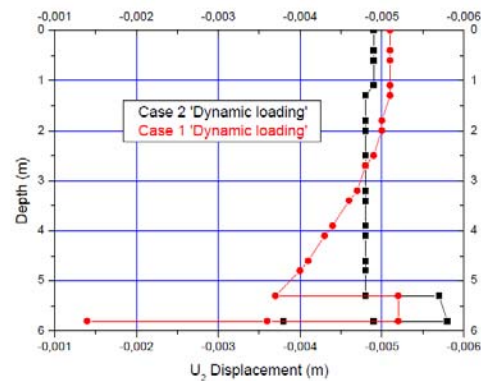


Fig. 12. Variation of U2 wall displacement with depth for seismic loading

VI. CONCLUSION

Analytical analyses and implicit and explicit numerical methods are used to compare results of cantilever retaining wall supporting waste tire reinforced sand to the results of the same cantilever retaining wall supporting only sand, under seismic loading of El Centro type. The following conclusions are drawn:

- According to the analytical computation, the safety factors for sliding as well as for overturning are less than the default minimum values for all cases.
- For the retaining wall supporting sand case: the lowest Von Mises stress value is about 9.7 kPa whereas the highest value is about 13.95 MPa and is observed in the wall between the base slab and the stem. The higher value of Von Mises stress for the dynamical case is 3.95 times higher compared to the static case.
- For the retaining wall supporting waste tire reinforced sand under static loading case: the Von Mises stress distribution changes in the range of 7.930 to 3465 kPa and the lowest values are observed near the ground level. Under El Centro excitation, the higher Von Mises stress (4.024 MPa) is observed between the base slab and the stem of the retaining wall in the soil cover zone. This value is 3.46 times lower compared to the retaining wall supporting sand with dynamic loading.
- For U1 and U2 displacements, the variations with depth are similar for each type of loading, but the values for the case of retaining wall supporting waste tire reinforced sand are slightly lower compared to the ones of the case of retaining wall supporting only sand.

REFERENCES

[1] C. Rothfuss, C. Y. Cha, "Utilization of a scrap tire-waste oil derived carbonous residue as an asphalt modifier", *Polymer Recycling*, Vol. 2, No. 3, pp. 201–212, 1996

[2] C. Y. Wang, J. H. Cheng, H. P. Shih, J. W. Chang, "Ring columns as pier scour countermeasures", *International Journal of Sediment Research*, Vol. 26, No. 3, pp. 353-363, 2011

- [3] H. Trouzine, A. Asroun, N. Asroun, F. Belabdelouahab, N. T. Long, "Problématique des pneus usés en Algérie", *Nature & Technologie*, Vol. 5, pp. 28-35, 2011 [in French]
- [4] N. T. Long, *Le Pneusol: Recherches-Réalisations-Perspectives*, Thèse de doctorat du LCPC, INSA Lyon, 1993 [in French]
- [5] M. R. Hausmann, "Slope remediation", *Proceedings of the Stability and Performance of Slopes and Embankments Conference*, ASCE Geotechnical Special Publication, Vol. 2, pp. 1274-1317, 1990
- [6] V. K. Garga, V. O'Shaughnessy, "Tire-reinforced earthfill. Part 1: Construction of a test fill, performance, and retaining wall design", *Canadian Geotechnical Journal*, Vol. 37, No. 1, pp. 75-96, 2000
- [7] V. O'Shaughnessy, V. K. Garga. "Tire-reinforced earthfill. Part 2: Pull-out behaviour and reinforced slope design", *Canadian Geotechnical Journal*, Vol. 37, No. 1, pp. 97-116, 2000
- [8] WYMCC, *Reuse of worn tyres in civil engineering construction*, Internal Report. West Yorkshire Metropolitan County Council, 1977
- [9] N. B. Romdhane, R. Nasri, M. Chaieb, N. T. Long, "Comportement dynamique du pneusol, Etude sur modèle réduit tridimensionnel, Essai sur table vibrante, Actes des 4eme Congres National AFPS, Saint-Rémy lés Chevreuse, France, 1996 [In French]
- [10] Y. Guillard, N.T. Long, P. Ursat, J. C. Valleur, "Pneusol : Essais de vibrations, Actes des 2eme Congres National AFPS, France, 1989 [In French]
- [11] S. L. Kramer, *Geotechnical earthquake engineering*, Englewood Cliffs, NJ: Prentice-Hall 1996
- [12] B. M. Basha, S. G. L. Babu, "Reliability assessment of internal stability of reinforced soil structures: A pseudo-dynamic approach", *Soil Dynamics and Earthquake Engineering*, Vol. 30, No. 5, pp. 336-353, 2010
- [13] D. Choudhury, S.M. Ahmad, "External stability of waterfront reinforced soil structures under seismic conditions using a pseudo-static approach", *Geosynthetics International*, Vol. 16, No.1, pp. 1-10, 2009
- [14] R. S. Steedman, X. Zeng, "The influence of phase on the calculation of pseudo-static earth pressure on a retaining wall", *Geotechnique*, Vol. 40, No. 1, pp. 103-112, 1990
- [15] A. K. Chopra, *Dynamics of structures theory and applications to Earthquake Engineering*, University of California at Berkeley, Prentice-Hall, 1995
- [16] H. B. Seed, R. V. Whitman, "Design of earth retaining structures for dynamic loads", *ASCE Specialty Conference on Lateral Stresses in the Ground and Design of Earth Retaining Structures*, pp. 103-147, USA, 1970
- [17] *ABAQUS User's Examples and Theory Manual*, Version 5.7. Hibbitt, Karlsson & Sorensen Inc., 1998
- [18] J. S. Sun, K. H. Lee, H. P. Lee, "Comparison of implicit and explicit finite element methods for dynamic problems", *Journal of Materials Processing Technology*, Vol. 105, No. 1-2, pp. 110-118, 2000
- [19] N. Rebelo, J. C. Nagtegaal, L. M. Taylor, R. Passmann, "Comparison of implicit and explicit finite element methods in the simulation of metal forming processes", *NUMIFORM 92, International Conference on Numerical Methods in Industrial Forming Processes*, pp. 99-108, 1992
- [20] Hibbitt, Karlsson & Sorensen Inc., "Application of implicit and explicit finite element techniques to metal forming", *Journal of Material Process Technology*. Vol. 45, pp. 649-656, 1994
- [21] T. J. R. Hughes, *The finite element method – linear static and dynamic element analysis*, Englewood Cliffs, (NJ): Prentice-Hall, 1987
- [22] T. Belytschko, W. K. Liu, B. Moran, *Nonlinear finite element for continua and structures*, Chichester: John Wiley & Sons Ltd, 2000
- [23] L. Siad, M. Ould Ouali, A. Benabbes, "Comparison of explicit and implicit finite element simulations of void growth and coalescence in porous ductile materials", *Materials and Design*, Vol. 29, No. 2, pp. 319-329, 2008